Available online at www.sciencedirect.com
SCIENCE DIRECT®
International Journal of Heat and Mass Transfer 49 (2006) 2820–2828
International Journal of HEAT and MASS TRANSFER
www.elsevier.com/locate/ijhmt

Onset of penetrative convection of cold water in a porous layer under mixed boundary conditions

A. Mahidjiba [a], L. Robillard [b,*], P. Vasseur [b]

[a] *Ouranos, 550 Sherbrooke West Street, 19th Floor, Montréal, Que., Canada H3A 1B9*
[b] *École Polytechnique de Montréal, C.P. 6079, Succ. 'Centre ville' Montréal, Que., Canada H3C 3A7*

Received 25 September 2005; received in revised form 16 February 2006
Available online 22 May 2006

Abstract

In the present work, the onset of convection in a two-dimensional horizontal porous layer saturated with cold water is studied numerically, using the linear stability analysis. The Dirichlet–Dirichlet, Neumann–Dirichlet and Dirichlet–Neumann thermal boundary conditions are applied on the horizontal walls of the cavity, respectively. Both the infinite and the confined layers are investigated. The finite element method is used to solve the linearized perturbation equations. The onset of convection is found to be dependent of the aspect ratio of the cavity, A and the inversion parameter, γ. The effect of these control parameters is studied for both infinite and finite layer cases. The effect of various thermal boundary conditions imposed on the horizontal layer is also investigated in this study.

Keywords: Penetrative convection; Density inversion; Porous medium; Dirichlet and Neumann boundary conditions; Linear stability; Finite and infinite layers

1. Introduction

Natural convection through porous media has been studied extensively in the past. A review of the literature (see for instance Nield and Bejan [1]) indicates that most of the studies were done with Boussinesq fluids, i.e., fluids exhibiting linear density as a function of temperature. However, water is known to feature an anomalous density–temperature relationship, the so-called density inversion phenomenon, having a maximum density at a temperature near 4 °C. In the past three decades, considerable interest has been focused on problems with density inversion because of applications in many fields such as geophysics and astrophysics.

Most works carried so far are concerned with the natural convection of pure cold water in a vertical enclosure. Watson [2] seems to be the first to demonstrate numerically convective flow reversals of cold water confined in a cavity differentially heated from the sides. Since this pioneering numerical work, this problem has received considerable attention. Representative work includes Vasseur and Robillard [3], Seki et al. [4,5], Inaba and Fukuda [6,7]. All these studies indicate that taking the density anomaly into account leads to peculiar behaviours, such as multicellular flow structure and heat transfer minima. A few studies were also concerned with the onset of motion in a horizontal fluid layer heated from below. Veronis [8] obtained, on the basis of the linear stability theory, the critical Rayleigh numbers in a fluid layer with 0 °C imposed at its bottom. Seki et al. [9,10] investigated rigid-rigid and free-rigid systems. The Galerkin's method was used by Merker et al. [11] to study instabilities in a cold layer of fluid. The non-linear stability was investigated by Malkus and Veronis [12].

A few studies have also been concerned with the problem of stability in a horizontal porous layer saturated with cold water. Using a cubic density–temperature

* Corresponding author. Tel.: +1 514 340 4711/4154; fax: +1 514 340 5917.
E-mail address: luc.robillard@polymtl.ca (L. Robillard).
URL: www.meca.polymtl.ca/convection (L. Robillard).

0017-9310/$ - see front matter © 2006 Elsevier Ltd. All rights reserved.
doi:10.1016/j.ijheatmasstransfer.2006.02.019

Nomenclature

A	aspect ratio, L'/H'
A_m	modified aspect ratio, L'/h'_{max}
H'	overall height of the layer
h'_{max}	height of the unstable layer in pure conduction
k	thermal conductivity of the saturated porous medium
L'	width of the porous layer
q'	imposed heat flux on the horizontal boundaries
R	Darcy Rayleigh number, $gKH'\beta_1\Delta T'^2/(\alpha\nu)$
R_l	standard Rayleigh number for linear convection, $gKH'\beta\Delta T'/(\alpha\nu)$
R_m	modified Darcy Rayleigh number, Eq. (6)
t	dimensionless time, $t'/(\sigma H'^2/\alpha)$
$\Delta T'$	temperature difference based on the overall depth of the layer in pure conduction, $q'H'/k$
T'_{max}	temperature corresponding to the density ρ_{max}, ($T'_{max} = 4\,^\circ C$)
(x, y)	dimensionless coordinate system, x'/H', y'/H'
(u, v)	dimensionless velocity terms, $u'/(\alpha/H')$, $v'/(\alpha/H')$

Greek symbols

α	thermal diffusivity, $k/(\rho_{max}C)_f$
β	thermal expansion coefficient, Eq. (13) $(^\circ C)^{-1}$
β_1	coefficient, Eq. (1) $(^\circ C)^{-2}$
γ	inversion parameter, $2(T'_{max} - T'_L)/\Delta T'$
λ	wavelength
$\bar{\lambda}$	eigenvalue
σ	heat capacity ratio, $(\rho_{max}C)_p/(\rho_{max}C)_f$
ν	kinematic viscosity of fluid
ρ	density of fluid
ρ_{max}	maximum density
$(\rho_{max}C)_f$	heat capacity of fluid
$(\rho_{max}C)_p$	heat capacity of saturated porous medium
Ψ	dimensionless stream function, Ψ'/α

Subscripts

c	critical value at incipient convection
m	modified value

Superscript

$'$	stands for dimensional variable

relationship, Sun et al. [13] were the first to predict the onset of convective flow. It was demonstrated experimentally by Yen [14] that the onset of motion, in a porous medium saturated with cold water, depends on parameters which are function of the boundary temperature. Relying on the linear stability theory, the effect of non-linear density on convection, in a porous medium has been conducted by Patil [15], for both Brinkman and Darcy models. A numerical study of two-dimensional natural convection in a horizontal porous layer heated from below and saturated with cold water has been performed by Blake et al. [16]. It was found that numerical results agree with linear stability results regarding the onset of convection. A theoretical investigation of the onset of thermal instabilities in the vicinity of the density maximum in the presence of a time-dependent non-linear mean temperature distribution within a porous layer was investigated by Poulikakos [17]. It was demonstrated that the dimensionless onset time decreases and the critical wave number increases as the Rayleigh number increases. Zhang [18] investigated numerically the problem of penetrative convection in a horizontal porous layer saturated with cold water. The existence of subcritical convection was demonstrated. The onset of convection in a horizontal porous cavity has been studied recently by Mamou et al. [19], on the basis of the Brinkman-extended Darcy model. The existence of multiple solutions for a given range of the governing parameters was demonstrated numerically, solving the full governing equations. Also, it was found that, when the upper stable layer extends over more than the half depth, subcritical convection is possible.

More recently, Mahidjiba et al. [20,21] studied the onset of convection in the case of a horizontal anisotropic porous layer of finite/infinite lateral extent, saturated with cold water. The existence of obliquely elongated convective cells, evenly distributed for the infinite layer was demonstrated. These cells result from the fusion of the primary convective cells (near lower boundary) and the secondary cells (near upper boundary).

The main purpose of this work is to study the onset of convection of an horizontal isotropic porous layer saturated with water at temperature near 4 °C. The influence of mixed boundary conditions applied on the horizontal walls of this layer is investigated. Such a condition, which can be encountered in many practical situations, has not been considered in the past, particularly in the case on the penetrative convection. Results obtained by linear stability analysis of finite and infinite layer for this case are presented.

2. Mathematical formulation

The problem under consideration is illustrated in Fig. 1. Uniform temperature T' is imposed on one of the two

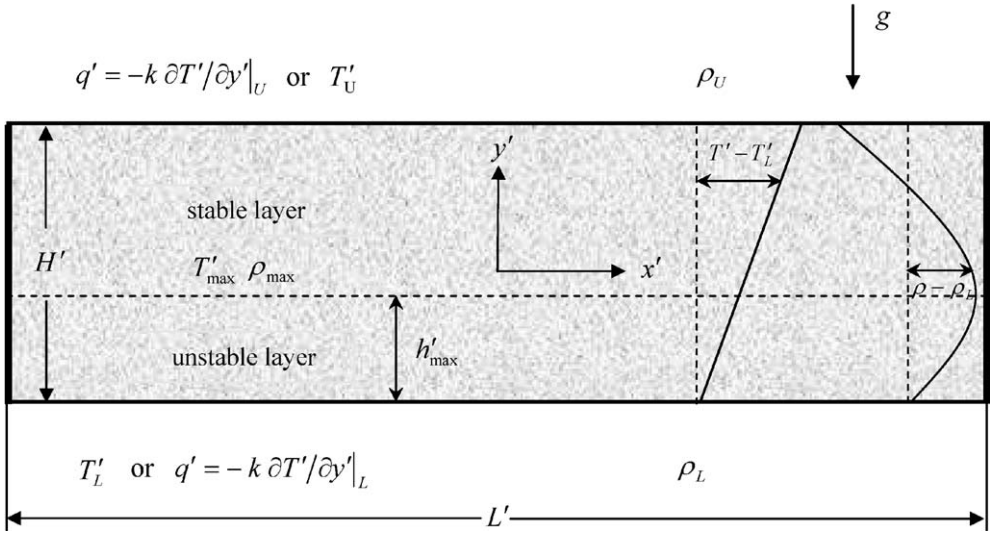

Fig. 1. Geometry of the physical problem: pure conduction conditions.

horizontal boundaries (Dirichlet condition) while a constant heat flux q' is applied to the other one (Neumann condition). The two vertical boundaries are subject to either adiabatic or periodic conditions respectively (those last conditions to be defined later), according to the type of layer (confined or unconfined) considered. When the temperature corresponding to the maximum density T'_{max} is somewhere between the two horizontal boundaries, temperature and density profiles corresponding to pure conduction heat transfer take the form given in Fig. 1 and the vertical position of the maximum density, ρ_{max} defines a separating line between a lower unstable region and a superposed stable one. It is to be noted that at, incipient convection, the dimensional temperature field obtained when only one of the horizontal boundaries is subject to a Dirichlet conditions (a Neumann condition being applied on the other one), remains identical in absolute value to the temperature field with Dirichlet boundary conditions imposed on both boundaries, uniform temperature T'_U and T'_L being obtained on upper and lower boundaries respectively.

The saturated porous layer is assumed to follow the Darcy law. The fluid density varies with temperature according to a parabolic relationship of the form

$$\frac{\rho - \rho_{max}}{\rho_{max}} = -\beta_1 (T' - T'_{max})^2 \tag{1}$$

with $T'_{max} = 3.98\ ^\circ C$ and $\beta_1 = 8 \times 10^{-6}\ (^\circ C)^{-2}$. The above relation was found to hold to within 4% over the range 0–8 °C, according to Moore and Weiss [22].

Since $q' = -k\partial T'/\partial y'$ on the boundary subject to a Neumann condition, the pure conduction temperature field gives

$$T'_U - T'_L = -\frac{q' H'}{k} = \Delta T' \tag{2}$$

with the characteristic steady state temperature $\Delta T'$ being positive or negative, according to the direction of q' (q' considered positive when upwards).

The particular relationship, Eq. (1), between density and temperature gives rise to two distinct cases that are to be considered in the present paper: Neumann condition applied to the upper boundary (case labelled ND) or applied to the lower boundary (case labelled DN), the other horizontal boundary being subject to a Dirichlet condition.

The dimensionless temperature is defined as follows:

$$T = \frac{T' - T'_L}{\Delta T'} \qquad \text{(ND)} \tag{3a}$$

$$T = \frac{T' - T'_U}{\Delta T'} + 1 \qquad \text{(DN)} \tag{3b}$$

This choice provides the same dimensionless temperature profile for both cases ND and DN with the dimensionless Neumann condition $\partial T/\partial y = 1$ applied on the relevant horizontal boundary.

Using H', $\alpha = k/(\rho_{max} C)_f$, α/H', $t'/(\sigma H'^2/\alpha)$ as respective scales for length, stream function, velocity and time, the dimensionless equations for momentum and energy (Mahidjiba et al. [20,21]) are

$$\frac{\partial^2 \Psi}{\partial x^2} + \frac{\partial^2 \Psi}{\partial y^2} = R(\gamma - 2T)\frac{\partial T}{\partial x} \tag{4}$$

$$\frac{\partial T}{\partial t} + u\frac{\partial T}{\partial x} + v\frac{\partial T}{\partial y} = \frac{\partial^2 T}{\partial x^2} + \frac{\partial^2 T}{\partial y^2} \tag{5}$$

where the stream function Ψ is related to the velocity by the usual relations $u = \partial\Psi/\partial y$ and $v = -\partial\Psi/\partial x$.

As usual, in deriving the governing equations (4) and (5), use has been made of the Boussinesq approximation. This latter is valid provided that density changes $\Delta\rho$ remain small in comparison of ρ_{max} (incompressible fluid) and temperature differences are small enough such that other properties of the saturated porous medium can be considered constant (see for instance Refs. [8,17]).

In the above equations, $R = gKH'\beta_1 \Delta T'^2/(\alpha\nu)$ is the Rayleigh number and $\gamma = 2(T'_{max} - T'_L)/\Delta T'$ (ND) or $\gamma = 2(T'_{max} - T'_U)/\Delta T' + 2$ (DN) is the inversion parameter.

Together with the aspect ratio $A = L'/H'$ defined in Fig. 1, they are the governing parameters of the present problem.

Whatever is the choice of the dimensional temperature imposed on one of the boundaries, the inversion parameter determines in pure steady state conduction the vertical position of T'_{max}, i.e., the vertical position of the maximum density, with h_{max}, the dimensionless thickness of the unstable layer, being equal to $\gamma/2$.

For the interpretation of the results, it is more appropriate to used a modified Rayleigh number R_m and a modified aspect ratio, A_m, both based on the depth h'_{max} of the unstable layer and on the difference of density $\Delta\rho_m$ across that layer, as defined for pure conduction heat transfer (Fig. 1). Thus the physical definition of the modified Rayleigh number remains the same

$$R_m = g\frac{Kh'_{max}}{\alpha\nu}\frac{\Delta\rho_m}{\rho_{max}} \tag{6}$$

although its mathematical expression changes, according to the vertical position of the maximum density in pure conduction. When the maximum density ρ_{max} lies between the two horizontal boundaries ($0 < \gamma \leqslant 2$), we have

$$\begin{aligned} h'_{max} &= H'(\gamma/2) \\ \frac{\Delta\rho_m}{\rho_{max}} &= \frac{\rho_{max}-\rho_L}{\rho_{max}} = \beta_1(T'_{max}-T'_L)^2 = \beta_1\Delta T'^2(\gamma/2)^2 \end{aligned} \tag{7}$$

When the maximum density is above the upper boundary ($\gamma \geqslant 2$), $h'_{max} = H'$ and we have

$$\frac{\Delta\rho_m}{\rho_{max}} = \frac{\rho_U-\rho_L}{\rho_{max}} = \frac{\rho_{max}-\rho_L}{\rho_{max}} - \frac{\rho_{max}-\rho_U}{\rho_{max}} \tag{8}$$

According to relationship (1), we obtain

$$\frac{\Delta\rho_m}{\rho_{max}} = \beta_1\left[(T'_{max}-T'_L)^2 - (T'_{max}-T'_U)^2\right] \tag{9}$$

which can be expressed as

$$\frac{\Delta\rho_m}{\rho_{max}} = \beta_1\left[2(T'_{max}-T'_L)(T'_U-T'_L) - (T'_U-T'_L)^2\right] \tag{10}$$

In pure conduction, $\Delta T' = T'_U - T'_L$, so that expression (8) gives

$$\frac{\Delta\rho_m}{\rho_{max}} = \beta_1\Delta T'^2(\gamma-1) \tag{11}$$

Therefore, from expression (7) and (11), the modified Rayleigh number and aspect ratio are

$$0 < \gamma \leqslant 2, \quad R_m = R(\gamma/2)^3, \quad A_m = A(\gamma/2)^{-1} \tag{12a}$$

$$\gamma \geqslant 2, \quad R_m = R(\gamma-1), \quad A_m = A \tag{12b}$$

On one hand, with $\gamma \gg 2$, the quadratic term in T of Eq. (4) becomes negligible and, since the thermal expansion coefficient β used in linear convection is related to β_1 (see, Robillard and Vasseur [3]) according to

$$\beta = 2\beta_1(T'_L - T'_{max}) \tag{13}$$

we obtain with $\gamma \gg 2$

$$R_m \approx R\gamma = \frac{gKH'}{\alpha\nu}\beta_1 2\Delta T'(T'_{max}-T'_L) = -\frac{gKH'\beta\Delta T'}{\alpha\nu} = R_l \tag{14}$$

R_l being the standard Rayleigh number for a linear density temperature relationship. This constitutes one of the asymptotic limits of the results to be presented. Thus, with $\gamma \to \infty$ the classic linear convection problem is obtained. On the other hand, there exists also, another asymptotic limit at $\gamma \to 0$, for which the (modified) Rayleigh number, as defined in (6), remains constant. For this other asymptotic case, the effect of the upper boundary is vanishing small, as it will be discussed later. It is to be noted that both definitions of R_m given in (12a,b) coincide when $\gamma = 2$. Such modified Rayleigh number and aspect ratio have already been used in previous articles by Mamou et al. [19] and Mahidjiba et al. [20,21].

On all solid boundaries, hydrodynamic boundary conditions are $\Psi = 0$, while the thermal boundary conditions are

$$x = \pm A/2, \qquad \partial T/\partial x = 0 \tag{15}$$

	DD	ND	DN
$y = -1/2$	$T = 0$	$T = 0$	$\partial T/\partial y = 1$
$y = +1/2$	$T = 1$	$\partial T/\partial y = 1$	$T = 1$

(16)

Strictly speaking, the above conditions are those of a confined layer. However, for the specific problem under concern, namely the case of a Darcy porous layer, results for the infinite layer are already contained in those of the confined layer. As a matter of fact, they correspond to the particular aspect ratio that minimizes the critical Rayleigh number. Alternatively, for the infinite layer, where the flow structure consists of periodic counter rotating cells, periodic boundary conditions in the x direction can be used to study the incipient convection, the aspect ratio A being limited to one wavelength λ. Those periodic conditions are defined as $\varphi(x,y) = \varphi(x+\lambda_c,y)$, where φ stands for any physical variable and λ_c corresponds to the critical wavelength.

3. Linear stability analysis

The method has been described in the past by Mahidjiba et al. [20,21] and only a brief description is presented here. The following transformations are introduced:

$$\Psi(x,y) = \Psi_R + \psi(x,y) \tag{17}$$

$$T(x,y) = T_R + \phi(x,y) \tag{18}$$

where $\Psi_R = 0$ and $T_R = y + 1/2$ correspond to the rest state and $\psi(x,y)$ and $\phi(x,y)$ are the perturbed solutions resulting from the convective effects.

3.1. Confined layer

Assuming separability, the steady perturbed solution can be written as follows:

$$\psi(x,y)=\psi_0 F(x,y) \quad \text{and} \quad \phi(x,y)=\phi_0 G(x,y) \tag{19}$$

where the amplitudes ψ_0 and ϕ_0 are small constants.

Substituting the rest-state solution and the small perturbations, Eqs. (17)–(19), into the governing equations (4) and (5) and discarding the second order terms involving the perturbations (at the beginning of convection, the amplitude ψ_0 and ϕ_0 are close to zero), the following linearized set of governing equations is obtained:

$$\psi_0\left(\frac{\partial^2}{\partial x^2}+\frac{\partial^2}{\partial y^2}\right)F = Rf(y)\phi_0\frac{\partial G}{\partial x} \tag{20}$$

$$-\psi_0\frac{\partial F}{\partial x}=\phi_0\left(\frac{\partial^2 G}{\partial x^2}+\frac{\partial^2 G}{\partial y^2}\right) \tag{21}$$

where $f(y)=\gamma-2y-1$.

The boundary conditions for F are similar to those of Ψ, except for $y=1/2$ where F takes the zero value. The function G also follows the boundary conditions for T.

The finite element method is employed to solve the above set of equations. The details of this method were already mentioned in the articles by Mahidjiba et al. [20,21]. After calculation and rearrangement of the terms, we obtain the following discretized set of linear equations

$$\psi_0[K_\psi]\{F\}=R\phi_0[B]\{G\} \tag{22}$$

$$\psi_0[L]\{F\}=\phi_0[K]\{G\} \tag{23}$$

where $[B]$, $[K_\psi]$, $[K]$ and $[L]$ are $m\times m$ square matrices with $m=4N_{\mathrm{n}}$, N_{n} being the total number of nodes, defined as $N_{\mathrm{n}}=(N_{\mathrm{e}x}+1)(N_{\mathrm{e}y}+1)$; $N_{\mathrm{e}x}$ and $N_{\mathrm{e}y}$ are the numbers of elements in x-direction and y-direction, respectively. The corresponding elementary matrices can be computed from the following integrals:

$$\begin{aligned}
[B]^{\mathrm{e}} &= -\int_{\Omega^e} f(y)\frac{\partial N_j}{\partial x}N_i\,\mathrm{d}\Omega^e,\\
[K]^e &= \int_{\Omega^e}\nabla N_j\cdot\nabla N_i\,\mathrm{d}\Omega^e,\\
[L]^e &= \int_{\Omega^e}\frac{\partial N_j}{\partial x}\cdot N_i\,\mathrm{d}\Omega^e,\\
[K_\psi]^e &= \int_{\Omega^e}\left(\frac{\partial N_j}{\partial x}\cdot\frac{\partial N_i}{\partial x}+\frac{\partial N_j}{\partial y}\cdot\frac{\partial N_i}{\partial y}\right)\mathrm{d}\Omega^e
\end{aligned} \tag{24}$$

where $N_j(y)$ are either the Lagrange interpolation functions for a quadratic case or the Hermite interpolation functions for the cubic case; $\{F\}$ and $\{G\}$ are solution vectors of length m.

It is noted that boundary integrals, known as the natural boundary conditions, vanish for the homogenous Dirichlet and Neumann boundary conditions. Eliminating ϕ_0 from Eqs. (22) and (23), we obtain the following eigenvalue problem equation:

$$\psi_0([E]-\bar{\lambda}[I])\{F\}=0, \quad \text{with} \quad [E]=[K_\psi]^{-1}[B][K]^{-1}[L] \tag{25}$$

and where $[I]$ is the identity matrix; $\bar{\lambda}=1/R$ represents the eigenvalue and $\{F\}$ the eigenvector.

The critical Rayleigh number for the onset of convection is given by $R_{\mathrm{C}}=1/\bar{\lambda}_{\max}$. The precision of the present numerical procedure depends, naturally, on the grid number.

3.2. Infinite layer

Eqs. (19), for the infinite layer case, become

$$\psi(x,y)=\psi_0 e^{i\omega x}F(y) \quad \text{and} \quad \phi(x,y)=\phi_0 e^{i\omega x}G(y) \tag{26}$$

where ω is the wavenumber defined as $\omega=2\pi/\lambda_{\mathrm{C}}$ and λ_{C} is the critical wavelength. Substituting the above expressions into the governing equations (4) and (5) and discarding the second order terms, the linearized governing equations are obtained as follows:

$$\psi_0\left(-a\omega^2F+i\omega b\frac{\partial F}{\partial y}+c\frac{\partial^2 F}{\partial y^2}\right)=i\omega R\phi_0 f(y)G \tag{27}$$

$$i\omega\psi_0 F=\phi_0\left(\omega^2 G-\frac{\partial^2 G}{\partial y^2}\right) \tag{28}$$

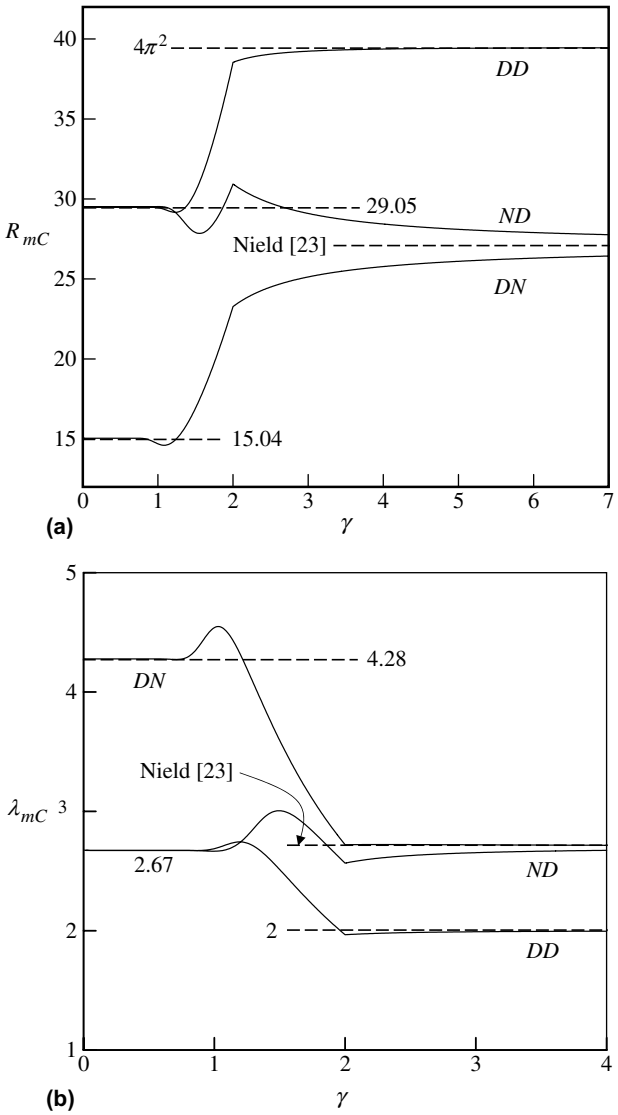

Fig. 2. Infinite layer: effect of the inversion parameter on (a) critical Rayleigh number, R_{mC} and (b) Critical wavelength, λ_{mC}.

While following the same process as for the confined layer case, we find the same eigenvalue problem equation. However, the matrices are now given by

$$
\begin{aligned}
[B]^e &= -\mathrm{i}\omega \int_{\Omega^e} f(y) N_j N_i \, \mathrm{d}\Omega^e, \\
[L]^e &= \mathrm{i}\omega \int_{\Omega^e} N_j N_i \, \mathrm{d}\Omega^e, \\
[K]^e &= \int_{\Omega^e} \left(\frac{\partial N_j}{\partial y} \frac{\partial N_i}{\partial y} + \omega^2 N_j N_i \right) \mathrm{d}\Omega^e, \\
[K_\psi]^e &= \int_{\Omega^e} \left(a\omega^2 N_j N_i + \frac{\partial N_j}{\partial y} \frac{\partial N_i}{\partial y} \right) \mathrm{d}\Omega^e
\end{aligned}
\tag{29}
$$

4. Results and discussion

All linear stability results at a specific γ and a given set of boundary conditions, DD, ND and DN, may be deduced from a single curve R_{mC} versus A_{m}, as computed from a confined layer containing a single incipient convective cell in the x-direction. The minimum R_{mC} obtained from the curve is the critical Rayleigh number of an infinite layer and the corresponding A_{m} represents the half wavelength λ_{mC}. For the case of a confined layer, critical Rayleigh numbers for n cells are obtained by scaling appropriately the single cell curve R_{mC} versus A_{m}.

4.1. Infinite layer

The critical Rayleigh number R_{mC}, defined in expressions (12a) and (12b) and the corresponding wavelength λ_{mC} are given as functions of the inversion parameter in Fig. 2a. As mentioned earlier, The curve labelled (DN) stands for the Neumann condition applied on the lower boundary and the Dirichlet condition applied on the upper boundary. Those conditions are interchanged between the two boundaries for the curve labelled (ND). The third curve (DD) for Dirichlet condition on both horizontal boundaries, is presented for comparison purpose. An asymptotic behaviour is found for $\gamma \gg 2$, for which the

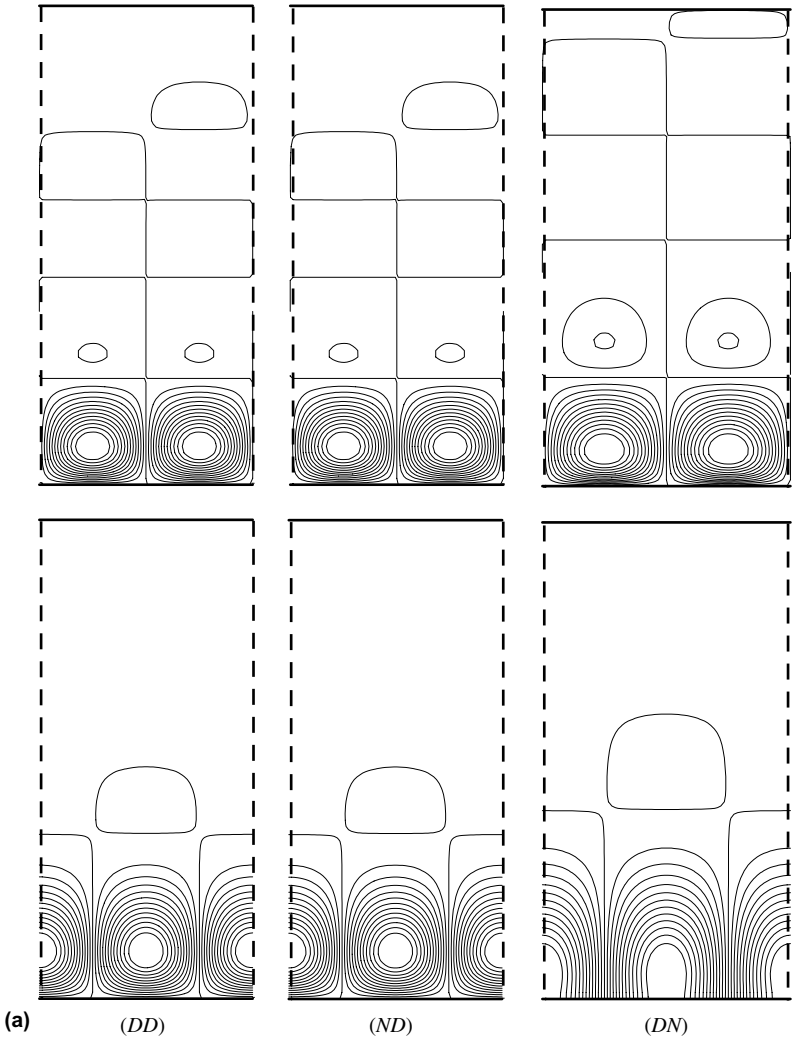

Fig. 3. Contour lines of the stream function and temperature profile for an infinite layer, for the three types of boundary conditions considered: (a) $\gamma = 1/3$, (b) $\gamma = 1/2$ and (c) $\gamma = 2$.

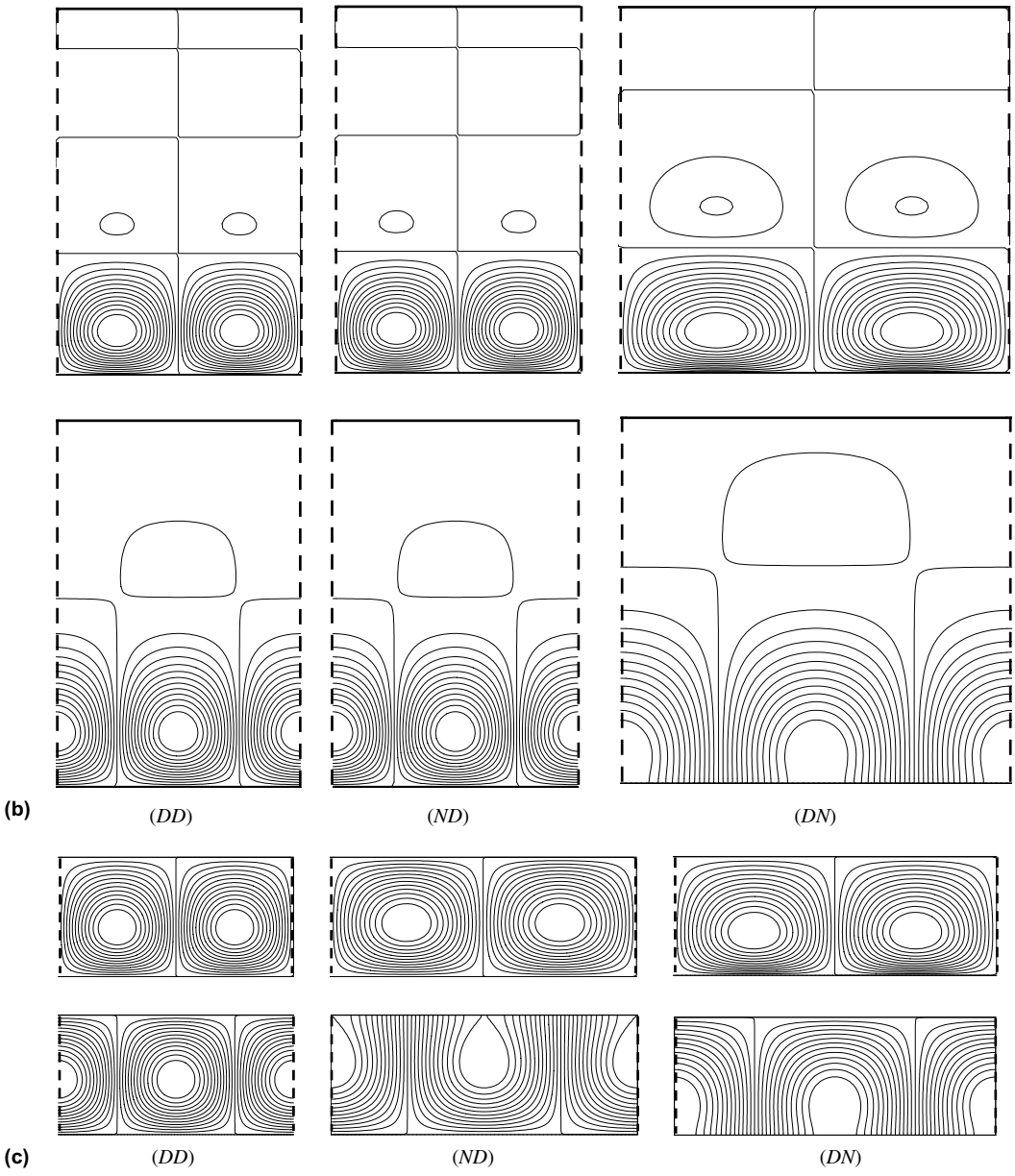

Fig. 3 (*continued*)

standard convection results (ρ and T linearly related) is recovered. In Fig. 2a, asymptotic values for R_{mC} are indicated by the two dashed lines with $R_{mC} = 4\pi^2$ for the (DD) curve. The two other curves, (ND) and (DN) tend toward the same limit $R_{mC} = 27.19$, as expected from symmetry considerations when ρ is linearly related to T. This critical Rayleigh number is in agreement with the value $R_{mC} = 27.10$ as reported by Nield [23]. With γ decreasing toward 2, the quadratic source term in Eq. (4) exerts its effect, either by decreasing (DD, DN) or increasing (ND) the critical Rayleigh number. At $\gamma = 2$, the abrupt change in behaviour characterizing all the curves corresponds to the change in the mathematical definition of R_{mC}, Eq. (12a,b). With γ decreasing below 2.0, the 4 °C isotherm (assuming a pure conduction temperature field), which appears first near the upper boundary, moves downward, creating an upper stable layer. A drastic drop characterizes all three curves at first, followed by a slight increase to an asymptotic value. Below $\gamma \approx 1$, the same asymptotic value $R_{mC} = 29.50$ is reached for the curves (DD) and (ND). The curve (DN) reaches a much lower value $R_{mC} = 15.04$ at $\gamma \approx 0.8$. This last asymptotic behaviour relies on the fact that, for γ decreasing from 2, the influence of the upper boundary on the flow behaviour at incipient convection is gradually reduced with the presence of the upper stable layer. At $\gamma \leqslant \sim 1$ (or $\sim$0.8), that influence becomes negligible. The threshold for incipient convection depends solely on the thickness of the unstable lower layer and on the density difference across that layer, both physical parameters on which R_{mC} is based. Thus, R_{mC} becomes constant and the curves (DD) and (ND), which differ only by their upper thermal boundary conditions, reach the same asymptotic

value. The abrupt change of slope observed at $\gamma = 2$, in Fig. 2a,b is merely due to the change of definition of both the modified Rayleigh number and wavelength, Eq. (12a,b). This approach allows one to obtain a finite asymptotic value when γ tends toward zero.

It is observed in Fig. 2b that the critical wavelength λ_{mC} increases quite markedly with the occurrence of a stable upper layer, i.e., with γ decreasing from 2. This is due to the fact that there is room offered by the stable layer for the expansion of the convective cells generated in the lower unstable layer. This behaviour is obvious in Fig. 3 which represents, for one wavelength of the infinite layer, incipient flow field (above) together with corresponding perturbations of the pure conduction temperature field (below). Those flow and temperature fields are represented respectively by streamlines and isotherms. For instance, in Fig. 3a, $\gamma = 1/3$ indicates that the unstable layer is limited to $H'/6$. Clearly for all the three cases DD, ND and DN, the flow field defining the lower cells extends in the upper direction beyond $H'/6$. The same behaviour is manifest for the set of flow fields shown in Fig. 3b for which the unstable layer thickness is $H'/4$. In Fig. 3a,b, the cases with Neumann boundary conditions applied to the lower boundary (DN) have a relatively larger critical wavelength and penetrate deeper into the stable layer.

For the three cases of Fig. 3c ($\gamma = 2$), there is no stable layer and the minimum density occurs at the upper boundary. For both cases ND and DN, the Neumann boundary condition gives rise to a large critical wavelength, in conformity with Fig. 2b.

4.2. Confined layer

The effect of lateral confinement on the critical Rayleigh R_{mC} is illustrated in Fig. 4 for $\gamma = 1/2$. The curve R_{mC} versus A_m shows a series of peaks distributed along the abscissa A_m. Each peak indicates that a new convective cell near the lower boundary is added to the flow field, with increasing A_m. The minimum value of R_{mC} between two successive peaks corresponds to the critical Rayleigh for the infinite layer. Those minimum values (29.05 and 15.04) shown by the dashed lines are in fact the ones shown at $\gamma = 1/2$ for DD or ND and DN respectively in Fig. 2a. It is to be noted that the flow field at those minimum values of R_{mC} is identical to the half wavelength of the flow patterns shown in Fig. 3, this half wavelength being repeated in the horizontal direction inside the cavity in accordance with the value of A_m.

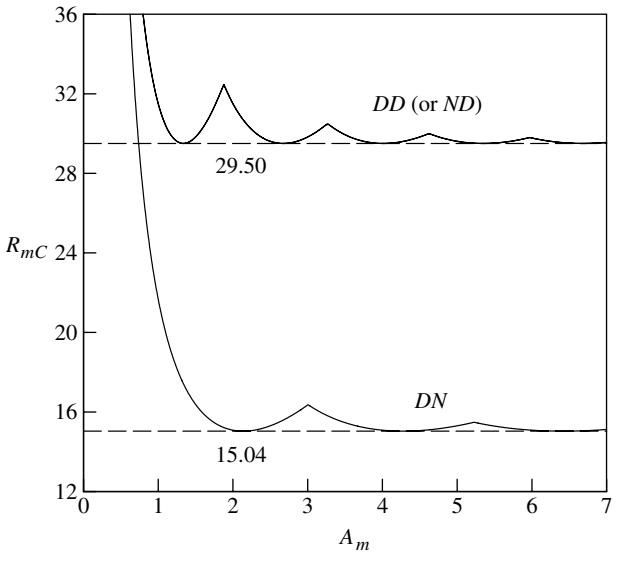

Fig. 4. Effect of the aspect ratio A_m, for a confined layer, on the critical number R_{mC} for the three types of boundary conditions considered ($\gamma = 1/2$).

5. Conclusion

Conditions at which incipient convection occurs have been studied for the case of a cold water saturated porous medium subject to a vertical temperature gradient. The layer of infinite extent as well as the laterally confined layer have been considered. Mixed Neumann and Dirichlet thermal boundary conditions were imposed on the horizontal boundaries, lateral boundaries for the confined layer being adiabatic.

An inversion parameter γ has been used to delimitate the part of the total depth occupied by the unstable layer. Critical Rayleigh numbers defining the threshold of convection have been established as functions of γ for the case of the infinite layer. Results indicate that an asymptotic situation is reached when $\gamma \leqslant 1$, for which the upper boundary conditions do not influence anymore the convective threshold. It has also been found that, with γ increasing above 2, the solutions reach asymptotically the classical case of a fluid with a linear density temperature relationship.

References

[1] D.A. Nield, A. Bejan, Convection in Porous Media, Spring Verlags, 1999.
[2] A. Watson, The effect of the inversion temperature on the convection of water in an enclosed rectangular cavity, Q. J. Mech. Appl. Math. 15 (1972) 423–446.
[3] L. Robillard, P. Vasseur, Effet du maximum de densité sur la convection libre de l'eau dans une cavité fermée, Can. J. Civil Eng. 6 (1979) 481–493.
[4] N. Seki, S. Fukusako, H. Inaba, Visual observation of natural convective flow in a narrow vertical cavity, J. Fluid Mech. 84 (1978) 695–704.
[5] N. Seki, S. Fukusako, H. Inaba, Free convection heat transfer with density inversion in a confined rectangular vessel, Warme-und Stoffubertragung 11 (1978) 145–156.
[6] H. Inaba, T. Fukuda, An experimental study of natural convection in an inclined rectangular cavity filled with water at its density extremum, J. Heat Transfer 106 (1984) 109–115.
[7] H. Inaba, T. Fukuda, Natural convection in an inclined square in regions of density inversion of water, J. Fluid Mech. 142 (1984) 363–381.
[8] G. Veronis, Penetrative convection, Astrophys. J. 137 (1963) 641–663.
[9] N. Seki, S. Fukusako, M. Sugawara, Free convective heat transfer and criterion of onset of free convection in horizontal melt layer of ice heated by upper rigid surface, Warme-und Stoffubertragung 10 (1977) 269–279.

[10] N. Seki, S. Fukusako, M. Sugawara, A criterion of onset of free convection in a horizontal melted layer with free surface, J. Heat Transfer 99 (1977) 92–98.
[11] G.P. Merker, P. Waas, U. Grigull, Onset of convection in a horizontal water layer with maximum density effects, Int. J. Heat Mass Transfer 22 (1979) 505–515.
[12] W.V.R. Malkus, G. Veronis, Finite amplitude cellular convection, J. Fluid Mech. 4 (1979) 225–260.
[13] Z.S. Sun, C. Tien, Y.C. Yen, Onset of convection in a porous medium containing liquid with a density maximum, in: Proceeding of the Fourth International Heat Transfer Conference, Paris, Versailles, NC 2 11, 1972.
[14] Y.C. Yen, Effects of density inversion on free convection heat transfer in a porous layer heated from below, Int. J. Heat Mass Transfer 17 (1974) 1349–1356.
[15] R. Patil, Convection in a porous medium with nonlinear density effects, Lett. Heat Mass Transfer 9 (1982) 131–140.
[16] K.R. Blake, D. Poulikakos, A. Bejan, Natural convection near 4 °C in a water saturated porous layer heated from below, Int. J. Heat Mass Transfer 27 (1984) 2355–2363.
[17] D. Poulikakos, Onset of convection in a horizontal porous layer saturated by cold water, Int. J. Heat Mass Transfer 28 (1985) 1899–1905.
[18] X. Zhang, Wave Number Selection in Penetrative Convection, Ph.D. Thesis, École Polytechnique de Montréal, Québec, Canada, 1989.
[19] M. Mamou, L. Robillard, P. Vasseur, Thermoconvective instability in a horizontal porous cavity saturated with cold water, Int. J. Heat Mass Transfer 42 (1999) 4487–4500.
[20] A. Mahidjiba, L. Robillard, P. Vasseur, Onset of convection in a horizontal anisotropic porous layer saturated with water near 4 °C, Int. Comm. Heat Mass Transfer 27 (6) (2000) 765–774.
[21] A. Mahidjiba, Convection Naturelle en Milieu Poreux Anisotrope-Effet du Maximum de Densité, Ph.D. Thesis, École Polytechnique de Montréal, Québec, Canada, 2001.
[22] D.R. Moore, N.O. Weiss, Nonlinear penetrative convection, J. Fluid Mech. 61 (1973) 553–581.
[23] D.A. Nield, Onset of thermohaline convection in a porous medium, Water Resour. Res. 11 (1998) 553–560.